Available online at www.sciencedirect.com

SCIENCE DIRECT®

Sedimentary Geology 171 (2004) 13–36

Sedimentary Geology

www.elsevier.com/locate/sedgeo

Evaluation of sediment provenance using magnetic mineral inclusions in clastic silicates: comparison with heavy mineral analysis

Mark W. Hounslow[a,*], Andrew C. Morton[b,c]

[a]CEMP, Geography Department, Lancaster Environment Centre, Lancaster University, Lancaster, LA1 4YW, UK
[b]HM Research Associates, 100 Main Street, Woodhouse Eaves, Leicestershire, LE12 8RZ, UK
[c]Department of Geology and Petroleum Geology, University of Aberdeen, Aberdeen, AB24 3UE, UK

Received 1 November 2003; received in revised form 1 March 2004; accepted 12 May 2004

Abstract

Magnetic Fe-oxide inclusions within framework clastic grains in sediments provide an indication of the provenance of the enclosing host silicate particles. Magnetic mineral inclusion characterisation is performed using a variety of magnetic properties that are related to magnetic mineral abundance, magnetic grain size (domain state), oxidation state and magnetic grain interaction. The magnetic methodology extends that based on a conventional set of environmental magnetic measurements. Using a variety of recent sediments, transported from known rock sources (within the UK and Eire), it is demonstrated, using discriminant function analysis, that the magnetic properties of the Fe-oxide inclusions provide a clear distinction of primary provenance. This is both at the large scale in terms of various gneiss, schist and granite sources and also at a smaller scale when considering subdivisions of these sources. Using case studies from the marine Upper Jurassic (Piper Formation) and non-marine Triassic sediments (Otter Bank Sandstone and Foula Sandstone Formations), it is shown that provenance differences, clearly expressed by the results of heavy mineral analysis, are also sensitively displayed by the magnetic mineral inclusion data. The provenance classification is based around use of hierarchical cluster analysis and multidimensional scaling. Simple statistical tools are developed to determine a least-noisy subset of magnetic parameters, which are most suitable for stratigraphic provenance discrimination. The Triassic case study has indicated the magnetic mineral inclusion technique is most sensitive when using the sediment fractions larger than 150 μm.

Keywords: Inclusions; Magnetic minerals; Provenance; Heavy minerals; Environmental magnetism; Magnetite; Fe-oxides; Hydrocarbon reservoirs

* Corresponding author.
E-mail address: m.hounslow@lancaster.ac.uk (M.W. Hounslow).

0037-0738/$ - see front matter © 2004 Elsevier B.V. All rights reserved.
doi:10.1016/j.sedgeo.2004.05.008

1. Introduction

Environmental magnetism is the study of the magnetic properties of natural Fe-oxides as a tool for understanding and interpreting the processes in sedimentary systems (Thompson and Oldfield, 1986; Maher et al., 1999; Evans and Heller, 2003). This works on the principle that the magnetic mineral measurements provide non-destructive and sensitive indicators of a wide variety of Fe-oxide properties (Dekkers, 1997). Environmental magnetism also provides one of a suite of mineral-based methods that allow stratigraphic correlation of sediments and can differentiate their provenance (Oldfield, 1991; Dekkers, 1997; Maher et al., 1999; Dearing, 2000). Mineral magnetic methods have been applied successfully in modelling sediment loads in fluvial systems, primarily through the characterisation of sedimentary source inputs (Oldfield et al., 1985; Caitcheon, 1998; Yu and Oldfield, 1993; Lees, 1999; Dearing, 2000). The methodology has also been used in characterising sediment provenance changes in glacial sediment systems (Walden et al., 1996).

Mineral magnetic methods rely on the presence of small amounts of Fe-oxides, many of which are detrital, as the principal carrier of the magnetic signal. Most consider these Fe-oxides to be dominated by discrete detrital particles, that is, the Fe-oxides are not significantly intergrown with non-magnetic phases (Thompson and Oldfield, 1986; Dekkers, 1997; Evans and Heller, 2003). Relative changes in Fe-oxide abundance, composition, grain size, grain shape, stress state and degree of grain magnetic interaction are reflected in differences in magnetic properties (Dunlop and Ozdemir, 1997; Walden et al., 1999). Such 'whole-sample' magnetic methods of sediment provenance evaluation have been mostly applied in Recent or Quaternary sediments (Walden et al., 1996; Dearing, 2000), and rarely applied to older sediments. This is mainly because the magnetic minerals most commonly used as the 'tracers' are magnetite and hematite, which can display mineralogical changes due to source to sink transport (Martinez-Monasterio et al., 2000) or diagenetic dissolution and sulfidization due to interactions with pore waters (Walker et al., 1981; Morad and Aldahan, 1986; Canfield and Berner, 1987; Karlin, 1990; Canfield et al., 1992; Hounslow et al., 1995). These discrete magnetic mineral grains, which may be altered by the action of aggressive pore fluids, are one type of grain association typically found in sediments (Vali et al., 1989; Hounslow and Maher, 1996).

The second type of grain association comprises Fe-oxides as magnetic mineral inclusions (MMI). These are often hosted in common detrital silicates, such as quartz and feldspar, but are also frequent in a wide variety of accessory silicate and other types of non-magnetic oxide particles (Hounslow and Maher, 1996, 1999). The MMI properties are typically dominated by low coercivity magnetic behaviour, which is commonly attributed to titanomagnetites with various composition and oxidation states, although probably frequently close to magnetite in composition. High coercivity phases such as haematite or goethite may also be important. These inclusions are frequently less than 10 μm in size, and are commonly submicron sized (Hounslow and Maher, 1996).

2. Origin of magnetic mineral inclusions

Folk (1974) recognised the significance of inclusions in clastic quartz and feldspar particles as potential markers for tracing sources. However, beyond this there is very little published work on the nature, morphology and composition of inclusions in clastic sedimentary particles, so inferences about the origin of magnetic mineral inclusions are largely drawn from the larger body of work that has been published from igneous and metamorphic rocks (Evans and Wayman, 1970; Morgan and Smith, 1981; Brearley and Champness, 1986; Geissman et al., 1988). These provide one potential source for such particles in sediments.

There are several possible pathways for Fe-oxide inclusions to form within monomineralic or composite host particles, and subsequently be liberated from the source rock, weathered and transported as a clastic particle.

(a) The Fe-oxides may grow as a sub-solidus product of host mineral equilibration. That is, the host exsolves the Fe-rich inclusion as part of the response to cooling (Morgan and Smith, 1981; Moseley, 1984; Schlinger and Veblen, 1989). The mineralogy, shape and size of the

inclusions are probably dictated by the host's Eh–pH conditions, lattice constraints and Fe-supply. Exsolution products are perhaps more typical of retrogressive phases in igneous and high-grade metamorphic rocks (Frost, 1991a).

(b) The inclusion may grow as a by-product of host-grain transformation to a new mineralogy, such as the decomposition of Fe-bearing silicates during weathering, heating, or the passage of fluids. Such transformations are perhaps most common during retrograde reactions in metamorphic rocks (Armbrustmacher and Banks, 1974; Morgan and Smith, 1981), although possible in other rock types (Reynolds et al., 1985; Otofuji et al., 2000). As with the exsolved case, the composition and morphology of the inclusion depends upon the environment of its host (Frost, 1991a).

(c) The host and inclusion may have formed at the same time, for instance in a mineral vein or volcanic glass (Heider et al., 1993) but the host's growth rate was larger than that of the inclusion. However, both reflect similar environmental conditions of formation.

(d) A ferrimagnetic grain may become enclosed by growth of an adjacent silicate phase, which captures the grain as an inclusion. Such behaviour may be typical of prograde reactions in metamorphic rocks, which display growth and redistribution of minerals. Such behaviour can also occur in sedimentary rocks by formation of quartz or feldspar overgrowths (over authigenic Fe-oxide phases such as haematite). In this case, the included grain's composition and morphology may not be so directly dependent upon its host.

While in the host, the inclusions may undergo transformations due to external environment changes, perhaps involving host-inclusion exchanges (cf. Frost, 1991b). The transformations of a silicate-hosted inclusion are likely to be limited while within the sedimentary environment, provided that the host does not allow leakage of external fluids. Consequently, the inclusion is likely to survive as long as the host survives in its environment. However, some common hosts such as amphiboles and pyroxenes are highly unstable during burial diagenesis; hence, changes related to burial and ensuing diagenesis are likely to be important in host preservation (Morton, 1984; Morad and Aldahan, 1986; Canfield et al., 1992). The pathways for inclusion production outlined above are very varied, and consequently the controls on the magnetic inclusion's composition, grain morphology, size and abundance are likely to be equally varied and specific to their environment of formation. Hence, they appear to be good potential indicators of sediment provenance.

The approach adopted here is twofold. Firstly, it is demonstrated that the MMI in clastic grain populations derived from different rock types during recent erosion (sample Set A) have different magnetic properties. This also provides some insight into the likely controls on the abundance, composition and grain size of the MMI. Secondly, using two case studies from deeply buried sediments (sample Set B) we show that likely provenance differences reflected in the MMI properties are retained after significant burial diagenesis. The changes in provenance are demonstrated by a parallel study of heavy minerals. These two methods represent different approaches to discrimination of provenance. Heavy mineral studies rely upon relative changes in mineralogy (and composition) of the accessory heavy mineral assemblages, which are separated from the light mineral fraction of the sediment. Magnetic inclusion properties are evaluated using the total grain population of the sample, since the inclusions are widely dispersed within the clastic grains. The linkage of the average magnetic properties to an 'average' grain composition, size, morphology and mineralogy is normally not possible because the properties derived from a magnetic grain population, and its magnetic behaviour, is dependent on several interrelated grain characteristics (Thompson and Oldfield, 1986; Dekkers, 1997; Maher et al., 1999).

3. Samples and methods

The locations, sample type and primary sources of sample Set A are indicated in Table 1. Sample Set A consists of modern river and beach sediments from areas of the UK and Eire in which clastic host grains are principally derived from erosion of igneous and metamorphic rocks (i.e. 'primary sources'). These Recent sediments have not been significantly con-

Table 1
Sample locations, sample types and primary rock source types for sample group A

Location	Rock source	Sample type	Rock group	*n*
Scilly Isles, UK	Variscan granite	beach	granite	4
Ox Mountains, Eire	Caledonian granite	river	granite	1
Guernsey, Channel Is., UK	Cadomian granites and granodiorites	beach	granite	3
Guernsey and Sark, Channel Is., UK	Icart and Cadomian gneisses	beach	gneiss	4
Lewis and Harris, NW Scotland[a]	Lewisian Gneiss	river and beach	gneiss	21
Harris, NW Scotland[a]	Lewisian Gneiss (South Harris Igneous Complex)	river	gneiss	6
NW Scotland[a]	Moine schists (Morar division)	river	schist	13
NW Scotland[a]	Moine schists (Loch Eil and Glenfinnan divisions)	river	schist	5
Co. Connemara and Mayo, Eire	Caledonian schists	beach	c. schists	3
Point of Sleat, Skye, Scotland	Caledonian schist	beach	c. schists	1
Various Connemara, Mayo, Eire	Silurian and Ordovician flysch	beach	lgm	3
St. Mawes Harbour, Cornwall, UK	Variscan slates	beach	lgm	1
Cromer Beach, Norfolk, UK	Vein quartz pebbles, from Quaternary tills	beach	vein quartz	8
Near Bakewell, Derbyshire, UK	Vein quartz pebbles, from Namurian sandstones	river	vein quartz	3
Alderley Edge, Cheshire, UK	Pebbles from Triassic (Sherwood Sandstone Group)	river	vein quartz	3
Mid Norfolk, UK	Quaternary reworked, Upper Cretaceous Chalk	river	chert	3
Ullapool and Durness, NW Scotland	Torridonian red beds	beach	red bed	2
Dawlish Warren and Exmouth Devon, UK	Permian/Triassic red beds	beach	red bed	2

The magnetic properties of these groups are summarised in Table 2.
[a] Indicates sample sets discussed by Morton et al. (2004). Lgm=low-grade metamorphic. *n*=number of samples analyzed.

taminated by tills from Quaternary long-distance glacial transport, and hence are principally derived from the local rock types. Examination of the rock fragments (larger than ~3 mm) in the sediments allowed visual validation of this.

Sample Set B comprises two separate case studies from hydrocarbon reservoir sandstones offshore Scotland. The first is from shallow marine sandstones of the Piper Formation (Oxfordian and Kimmeridgian) from the Ivanhoe/Rob Roy Field, well 15/21a-33 (Witch Ground Graben, Moray Firth). The second is from fluvial sandstones of the Otter Bank Sandstone and Foula Sandstone formations (early-middle Triassic) of the Strathmore Field, well (East Solan Basin, west of Shetland).

3.1. Magnetic mineral methods

Since the Fe-oxide inclusions could potentially modify the average density of the host grain, all magnetic measurements are performed on separate size fractions. This approach is comparable to that used in heavy mineral analysis, because it reduces the effects of hydrodynamic size sorting (Morton and Hallsworth, 1994, 1999). For sample Set A, the sediment was wet sieved in its native state into >500, 250–500, 150–250 and 38–150 μm grain size fractions. For Set B, this size separation was performed after acid treatment (as described below).

To remove the discrete Fe-oxide particles and obtain only those particle hosts with Fe-oxide inclusions, the samples were treated to 20 min in 100 ml of boiling concentrated (36%) HCl. Trials, using test samples simulating discrete magnetic oxides, showed that this preferentially removed the discrete magnetic components due to magnetite, ilmenite and magnetite (Alekseeva and Hounslow, 2004). This treatment also removes potential hosts that are soluble in HCl. For Set B, prior to acid treatment, samples were gently broken into pea-sized pieces and those with significant amounts of oil were pre-treated with 40 ml of 30% hydrogen peroxide overnight. Those with common carbonate (in both Set A and B) were pre-treated with 10% cold HCl until reaction ceased. For Set B, ultrasonic treatment was used for several minutes to disaggregate the sandstones prior to acid treatment. After acid treatment and sieving, the sized fractions were packed into 12 cc plastic containers suitable for the magnetic measurements (Walden et al., 1999).

The samples were subjected to a conventional set of magnetic measurements (Walden et al., 1999;

Maher et al., 1999). Magnetic susceptibility (χ) was measured using a Bartington MS2 susceptibility meter or an Agico KLY3 susceptibility meter. Anhysteretic remanent magnetisations (ARM) were applied using a DC field of 0.08 mT and an alternating field of 80 mT, and converted to susceptibility of ARM (χ_{ARM}). For a subset of samples, the ARM was subsequently demagnetised at 40 mT, using static demagnetisation along the ARM axis to give the percentage of ARM remaining (%d.ARM$_{-40\ mT}$). ARM is particularly strongly acquired in magnetite with single-domain behaviour (i.e. physical grain sizes of about 0.03 to 0.2 μm), and less strongly in larger magnetite particles. Backfield Isothermal Remanent Magnetisation (IRM) was applied using 20, 50, 100 and 300 mT fields (pulse magnetiser), after a saturation IRM (SIRM) at 1000 mT, using an electromagnet (Walden et al., 1999). These were converted to mass specific IRMs (i.e. IRM$_{20\ mT}$, IRM$_{50\ mT}$, IRM$_{100\ mT}$, IRM$_{300\ mT}$), the percentage of IRM acquired in the backfield coercivity increments (i.e. % IRM$_{0–20\ mT}$, %IRM$_{20–50\ mT}$, %IRM$_{50–100\ mT}$, %IRM$_{100–300\ mT}$, %IRM$_{0.3–1T}$) and the S-ratio (2*IRM$_{100\ mT}$/SIRM). The parameter χ_{HIRM} is also used, which is a measure of the amount of IRM acquired between 0.3 T and the SIRM, normalised by the field increment (0.7 T) in A m^{-1}. This is an approximate measure of the abundance of haematite or goethite. The resulting magnetisations were measured on a GM400 cryogenic magnetometer for the ARMs and a Molspin magnetometer for the IRMs. Both these machines were cross-calibrated. All measurements were corrected for the magnetic signal of the plastic containers. Limited starting sample mass of some samples precluded reliable magnetic measurements on some grain size fractions (i.e. those with mass <2 g). Most magnetic measurements were performed on grain-sized fractions of about 10–12 g. To compare the MMI provenance characteristics, the magnetic properties were compared between the same sieved host size fractions.

3.2. Heavy mineral methods

The heavy mineral data take two forms, conventional data and garnet geochemical data. Conventional heavy mineral data were acquired on the 63–125 μm fraction using a polarising microscope. In addition to determining the relative abundance of non-opaque detrital phases, a number of specific mineral ratios were determined. These include apatite/tourmaline, garnet/zircon, rutile/zircon, monazite/zircon and chrome spinel/zircon, and are denoted as index values of ATi, GZi, RuZi, MZi and CZi, respectively. These indices are relatively insensitive to changes in hydraulic conditions or diagenesis (Morton and Hallsworth, 1994) and are therefore considered to reflect source characteristics. Garnet geochemical data were acquired using a Link Systems AN10000 energy-dispersive X-ray analyser, attached to a Microscan V electron microprobe, following the method described by Morton (1985).

3.3. Statistical methods

Various multivariate statistical methods were used on the two magnetic data sets. Prior to analysis all magnetic parameters were checked for normality using the Kolmogorov–Smirnov statistic (Rock, 1988), and converted to $\log_{10}$ of the parameter, if the parameter data was better represented by a log-normal distribution. Normally distributed data is a general requirement for many multivariate statistics.

Discriminant function analysis (DFA) was used on sample Set A. The purpose here was to determine which magnetic parameters (if any) could be used to correctly classify the samples into their pre-determined source groupings. This used a selection procedure for the magnetic variables which minimised Wilks' lambda (also called the *U*-statistic) and a stepwise variable selection procedure based on the *F*-statistic (Rock, 1988; Manly, 1994).

Hierarchical cluster analysis (HCA) was used on sample Set B, for determining the membership of groupings of samples with similar sets of magnetic properties (Manly, 1994). In the HCA, Ward's cluster formation method was used, because it is recommended by Lees (1999) and shown by Milligan (1980) to be fairly typical in its response to data noise. Multi-dimensional scaling (MDS) was also used on sample Set B, using the same set of variables as the hierarchical cluster analysis, as a visual means of examining the between-cluster relationships and the robustness of the clusters (Minchin, 1987; Rock, 1988; Pentecost, 1999). A two-dimensional MDS analysis was used, with Euclidean distances for the

similarity matrix. Prior to both the HCA and MDS analyses on the sample sets, all the data were converted to *Z*-scores (i.e. mean of 0 and S.D. of 1). The cluster analysis and discriminant function analysis was performed using SPSS version 10.

4. Results for sample Set A

With sample Set A, our goal was to identify if there are differences in the MMI properties between rocks derived from different primary sources, and to establish which magnetic parameters might be most important in this distinction. This would, (a) determine if MMI properties could discriminate between sediment sources, and (b) contribute to an understanding of possible factors in the physical and chemical environment that might control the MMI differences. In order to do this objectively, discriminant function analysis (DFA) was utilised. The inputs to DFA were the sample groupings based on the type of primary sources from which the samples were derived, as well as the magnetic characteristics of each sample from these sources. The DFA attempts to find discriminant functions, using linear combinations of the magnetic parameters, which can reproduce the primary source groupings, using only the magnetic properties (Rock, 1988; Manly, 1994). The degree of success in using the MMI properties for this classification is a reflection of how distinctive the magnetic properties of these primary sources are. The DFA was applied using either the whole of the data from sample Set A, or subsets of these data. The three subsets were (1) schist and gneisses, (2) only schist sources (three types) and (3) the two granite groupings (Tables 1 and 2).

The DFA for the whole data set indicated that three magnetic parameters ($\log(\chi_{ARM})$, $IRM_{0.3\ T}$/SIRM and $\%IRM_{0.05–0.1\ T}/\%IRM_{0.1–0.3\ T}$) contributed to three canonical discriminant functions that maximised the correct classification of the data. Two of these parameters indicate that abundances of fine-grained magnetite (χ_{ARM}) and relative haematite (or goethite) content ($IRM_{0.3\ T}$/SIRM) are important mineralogical discriminators in this system. The third parameter ($\%IRM_{0.05–0.1\ T}/\%IRM_{0.1–0.3\ T}$) indicates the shape of the backfield IRM curve at high coercivities near the saturation of magnetite at 0.1–0.3 T. This parameter will be sensitive to a variety of properties including the magnetic grain size distribution, the magnetic grain interaction, the presence of elongate magnetic particles and the presence of magnetically soft (i.e. coercivity <0.3 T) haematite (Thompson and Oldfield, 1986; Walden et al., 1999; Evans and Heller, 2003).

The canonical discriminant functions classify correctly 61% of the samples. If the data were totally non-discriminating with respect to the primary rock sources, only about 8% of the data would be classified correctly. This indicates that there are strong differences in the MMI properties between primary sources. This classification is best for gneisses from NW Scotland (96%), Moine schists from NW Scotland (64%), vein quartz (71%), chert (100%) and granites (50%). The visual expression of the first two canonical discriminant functions clearly shows the division of these groups into mostly non-overlapping fields (Fig. 1). The separation for canonical discriminant function 1 is mainly based on $\log(\chi_{ARM})$ and $IRM_{0.3\ T}$/SIRM which separate gneisses from the vein quartz and chert. Vein quartz and chert have low χ_{ARM} and $IRM_{0.3\ T}$/SIRM, whereas gneisses have mostly large values of these parameters (Table 2). The canonical discriminant function 2 is contributed approximately equally by all three magnetic parameters, with high values of function 2 mostly due to large values of $\%IRM_{0.05–0.1\ T}/\%IRM_{0.1–0.3\ T}$ and low values of χ_{ARM} (Fig. 1). Low values of function 2 are mostly due to large values of $IRM_{0.3\ T}$/SIRM and low values of the other two parameters (Fig. 1).

The main mineralogical source of this variation in the data set is therefore expressed by the abundance of fine-grained magnetite, which contributes to the χ_{ARM} signal and is mainly responsible for the distinction into gneiss fields, which have χ_{ARM} greater than about 10×10^{-8} m^3/kg, and chert and quartz-vein fields, which have χ_{ARM} less than 0.5×10^{-8} m^3/kg (Table 2). The samples from the Moine schist sources have intermediate values of $1.2–2.4\times10^{-8}$ m^3/kg, with other groups (low grade metamorphic, red beds and Caledonian schists) intermediate between the gneiss field and the Moine Schist field (Fig. 1; Table 2).

The DFA for the schist and gneiss subset, selected $\log(\chi_{ARM})$ and $IRM_{0.3\ T}$/SIRM as the best parameters for discrimination. The two canonical discriminant functions allows separation into two main fields, one of mostly gneisses and the other of schist sources, plus

subregions corresponding to groupings of gneisses and schists from separate origins (Fig. 2). Overall, the discriminant functions classify 69% of the sample groups correctly into their respective source groups. The separation of the various schist sources is mainly due to $IRM_{0.3\ T}$/SIRM in canonical discriminant function 2, with the Glenfinnan and Loch Eil schists having a mean of 0.77, compared to the Morar schist of 0.61 (Table 2; Fig. 2). The $IRM_{0.3\ T}$/SIRM is a measure of the relative amount of haematite (or goethite) compared to magnetite.

Using DFA on the granite subset indicates that the best discrimination is performed with $d.ARM_{-40\ mT}$. This allows correct discrimination of 88% of the data, with the Variscan granites having a mean $d.ARM_{-40\ mT}$ of 31% and the Cadomian/Caledonian granites a mean value of 55% (Table 2).

In terms of magnetic mineral abundance, expressed by the SIRM (Table 2), the gneiss units have the largest concentrations of MMI from data Set A, with values mostly $>9\times10^{-5}$ A m^2/kg. The gneisses also have <10% of IRM acquired above 0.3 T (i.e. $\%IRM_{0.3-1\ T}$). Hence, we infer that the MMI magnetic properties of gneiss units are dominated by Fe-rich magnetic spinels such as magnetite (these type of magnetic properties are hereafter called magnetite-like properties). By contrast, the magnetic properties of vein quartz and chert are dominated by haematite or goethite, evident by the high values of $\%IRM_{0.3-1\ T}$ in excess of 40% (Table 2). The Moine schists and the red bed samples fall into a group with intermediate amounts of haematite or goethite, evident by $\%IRM_{0.3-1\ T}$ between 15% and 25% (Table 2). The dominance of the magnetite-like properties in the low grade metamorphic and red-beds is probably due to inheritance of most of the MMI from pre-existing grains.

The results from sample Set A indicate four main findings:

- There is separation into rock-type fields (e.g. gneiss, schist) that indicates the thermal and stress history might play an important control on the MMI properties.
- Both gneiss and schist fields (Fig. 2) can be separated into different tectonic and lithological

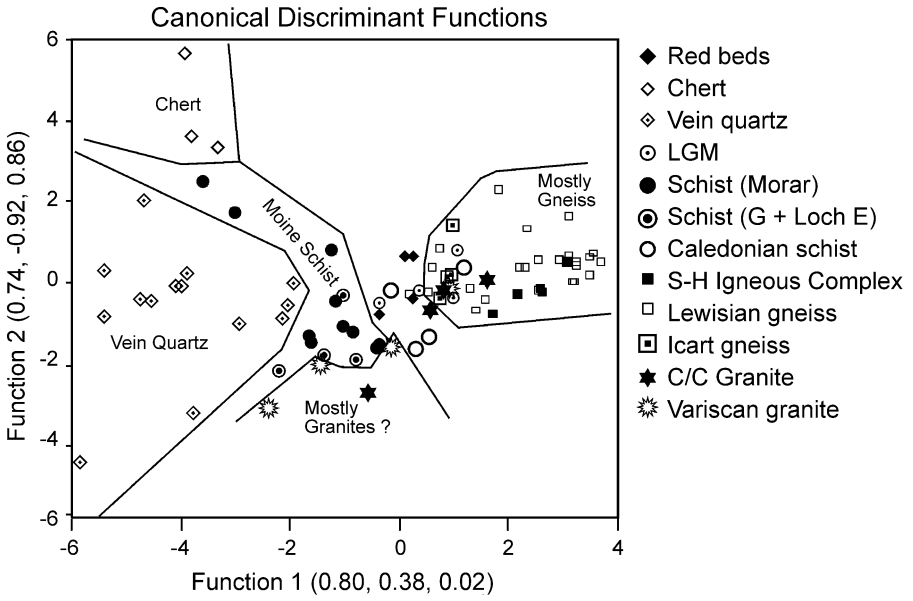

Fig. 1. Discriminant function plot for sample set A. The *x* and *y* axes are the canonical discriminant functions determined by the analysis. The numbers in brackets on each of these axes refer to the normalized coefficients associated with the three magnetic parameters ($\log(\chi_{ARM})$, $IRM_{0.3\ T}$/SIRM and $\%IRM_{0.05-0.1\ T}/\%IRM_{0.1-0.3\ T}$). The magnitude of these coefficients indicates the relative contribution to each of the respective functions on the *x* and *y* axes. The sample divisions are those in Table 1. The lines on the plot are simply drawn around fields of the same groups of samples and are not the boundaries defined by the discriminant function analysis.

Table 2
Mean values of magnetic inclusion properties for recent sediments sourced from locations indicated in Table 1

Source	N	χ_{lf} $\times10^{-7}$ m^3/kg	SIRM[a] $\times10^{-5}$ Am^2/kg	χ_{ARM}[a] $\times10^{-8}$ m^3/kg	%d.ARM$_{-40\ mT}$[a]	%IRM$_{0-20\ mT}$	%IRM$_{0.1-0.3\ T}$	%IRM$_{0.3-1\ T}$	IRM$_{0.3T}$/SIRM	%IRM$_{50-100\ T}$/%IRM$_{0.1-0.3\ T}$	χ_{ARM}/SIRM $\times10^{-3}$ m/A
Cadomian/Caledonian granites	4	0.17	8.08	7.76	54.8	19.5	20.9	9.9	0.918	1.098	0.76
Variscan granites	4	0.043	3.85	1.6	31.1	17.2	21.5	14.8	0.857	0.994	0.38
Icart Gneiss	4	0.287	9.88	9.3	42.1	21.2	16.5	9.1	0.904	1.474	0.80
Lewisian Gneiss	22	1.40	59.6	123.2	57.1	14.8	32.0	4.1	0.921	0.934	1.42
South Harris Igneous Complex	5	1.20	44.9	78.4	52.2	15.1	32.2	2.3	0.955	0.832	1.10
Caledonian schists	4	0.12	4.90	4.8	50.1	19.1	21.0	7.5	0.919	1.23	0.95
Moine schist (Glenfinnan+Loch Eil divisions)	5	0.29	5.03	1.16	48.6	17.6	25.8	16.7	0.767	0.846	0.31
Moine schist (Morar division)	12	0.46	7.10	2.35	47.0	13.9	30.1	20.5	0.607	0.773	0.50
Low-grade metamorphic	4	0.14	5.8	6.9	43.8	20.3	17.6	8.5	0.914	1.484	0.76
Vein quartz	14	−0.05	0.57	0.06	43.0	10.4	13.4	49.6	0.485	0.992	0.16
Chert	3	−0.02	0.55	0.27	28.1	8.9	3.7	69.4	0.32	2.21	0.48
Red beds	4	0.06	13.0	9.4	49.7	14.5	19.2	24.4	0.78	1.06	0.90

Some source groups in Table 1 have been combined.
[a] Indicates a log mean was determined.

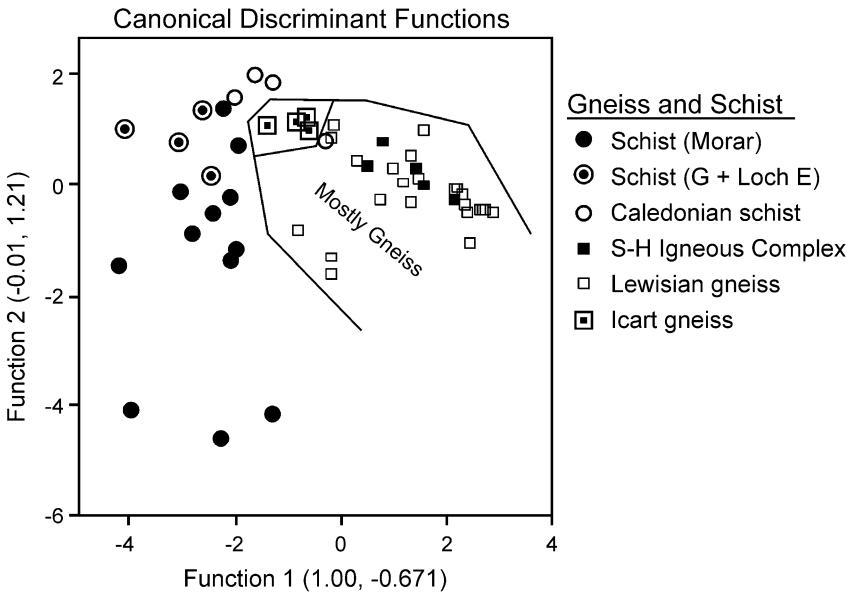

Fig. 2. Discriminant function plot for schists and gneisses from sample set A, with the canonical discriminant functions identified by the DFA. Normalized coefficients of $\log(\chi_{ARM})$, $IRM_{0.3\ T}$/SIRM are shown in brackets for each axis. The sample divisions are those in Table 1. The lines on the plot are simply drawn around fields of the same groups of samples and are not the boundaries defined by the discriminant function analysis.

units. This may indicate that the microchemical conditions within separate schist or gneiss units play a role in determining how the magnetic inclusions are formed. This is to some extent expected considering the various MMI pathways considered in Section 2.

- Low-temperature reactions in sedimentary or low-grade metamorphic rocks are probably insufficient to reset the MMI properties, so that part of the magnetic signal is likely to be inherited from the older rock sources from which these units are derived.
- Low-temperature systems responsible for production of chert and vein quartz appear to be characteristically dominated by haematite (or goethite) MMI production.

5. Results for sample Set B

The two case studies comprising Set B are significantly different from the samples in sample Set A, in that (a) the successions have been subjected to significant burial and associated diagenesis, and (b) there is no a priori information about provenance differences, other than that derived from analysis of the mineralogy of the units concerned. For both of these case studies, provenance information is provided by heavy mineral data, which enable an evaluation of the sensitivity of the MMI properties to provenance differences. In both case studies, samples were collected from sandstone successions with ranges in stratigraphic age, so that any provenance differences detected are related to switching of source areas.

5.1. Statistical analysis

The purpose of the DFA analysis when applied to sample Set A was to select magnetic variables that allow the best prediction of sediment source groupings based on prior knowledge of those groupings. In contrast, for sample Set B, potential differences in sediment provenance were evaluated using the MMI properties themselves. Cluster analysis provides a statistical tool to group samples with similar sediment provenance on the basis of their MMI properties. Cluster analysis classifies samples into groups with similar sets of properties, and provides measures of the similarity between these groups. Cluster analysis was applied to the MMI magnetic data using the

various proxies for magnetic abundance, magnetic grain size, composition and grain interaction.

The desired primary outcome of the analysis was an understanding of stratigraphic changes in provenance. Ideally, therefore, the cluster analysis would generate sample groupings that define some kind of time-related (stratigraphic depth) zonation of the MMI magnetic properties. However, the cluster analysis knows nothing about the stratigraphic order of horizons. Hence, stratigraphically adjacent samples belonging to a single cluster class indicate a high degree of stratigraphic coherency in the magnetic properties.

With multivariate data sets, it is good practice to utilise a priori information to select a subset of variables that are most powerful for discrimination using cluster analysis, while having the lowest inherent noise (Fowlkes et al., 1988; Manly, 1994; Lees, 1999; Rowan and Goodwill, 2000). This noise might include measurement, sampling or natural property variability. Inspection of the data might allow a qualitative way of gauging this noise in the magnetic variables, enabling pre-selection of variables for the cluster analysis. However, this would clearly be subjective, so the following quantitative procedure was developed in order to pre-select those variables most suitable as input to the cluster analysis.

The degree of down-hole 'noisiness' response for each variable was evaluated using what we have termed the stratal consistency function (SCF). This is the Pearson correlation coefficient (r) derived by the cross correlation between two subsets, P and Q, from each magnetic variable (X_{1-n}), where $P_{1,\ n-1}$ is the subset $X_{1,\ n-1}$ and $Q_{1,\ n-1}$ the subset $X_{2,n}$. A value of this function close to one indicates that adjacent horizons have similar magnitudes, whose difference is small compared to the variance in this variable. A value close to zero indicates that the difference between adjacent horizons is comparable in size to the variance in this variable. The SCF value is independent of the magnitude of the variable concerned, but is dependent to some extend on the normality of the variable. Log-normally distributed data variables often give lower values than the equivalent normally distributed data. Consequently, the SCF value can be used to pre-select certain magnetic parameters, according to how different they are from random noise. A statistical simulation (Ross, 1996) using 1000 sets of 32 sequential random numbers indicated a 95% percentile value of SCF of 0.36% and a 99% value of 0.46. This in essence means that in a data set with 32 sequential stratigraphic data points, the SCF value should be in excess of 0.36% to be 95% certain that the data set is not random (and SCF=0.46 for 99%). Considering this is a non-exhaustive simulation and our two magnetic case studies have 34 and 30 sampling points, we conservatively choose variables with an SCF value of $\geq|0.4|$ as being least likely to be strongly noisy (Table 3). These variables were flagged as potentially pre-selected for the cluster analysis.

5.2. Case study 1: the Piper Formation, well 15/21a-33

The Upper Jurassic Piper Formation in well 15/21a-33 (Ivanhoe/Rob Roy area, Outer Moray Firth, UKCS) contains two sandstone developments, the Piper Sandstone Member and the underlying Scott Sandstone Member. These units equate with the Supra Piper and Main Piper of Parker (1991), respectively. The Piper Formation consists of lower to upper shoreface sands with subsidiary distributary channel and washover sands. Boote and Gustav (1987) and

Table 3
Summary of magnetic properties for the MMI provenance clusters for samples from the Piper and Scott sandstones, Well 15/21a-33 (sand fraction 150–250 μm)

MMI cluster	N	SIRM[a] $\times10^{-5}$ Am^2/kg	χ_{ARM}[a] $\times10^{-8}$ m^3/kg	χ_{lf} $\times10^{-7}$ m^3/kg	$\%IRM_{0-20\ mT}$	$\%IRM_{20-50\ mT}$	$\chi_{ARM}/SIRM$ $\times10^{-3}$ m/A
PA	13	2.87	0.76	−0.02	20.0	33.0	0.52
PB_1	10	2.03	4.85	0.09	33.4	26.4	2.44
PB_2	10	3.92	7.59	0.33	32.9	26.1	2.10
SCF	33	0.41	0.25	0.24	0.30	0.47	0.46

[a] Indicates a log mean was determined. SCF=stratal consistency function.

Parker (1991) considered that the sands were deposited by a northward-prograding wave-dominated delta, but O'Driscoll et al. (1990) invoked the involvement of another source, lying to the northeast. Morton and Hallsworth (1994) demonstrated the involvement of two distinct sources, one characterising the Scott Sandstone and the other characterising the Piper Sandstone. The differentiation of the two sandstones can be made on the basis of both provenance-sensitive heavy mineral ratio data and garnet geochemistry. The Scott Sandstone has consistently lower apatite-tourmaline index (ATi), monazite-zircon index (MZi) and rutile-zircon index (RuZi) compared with the Piper Sandstone (Fig. 3). The means of the four heavy mineral indices for the two sandstone units are significantly different at the 95% level. Garnet assemblages in the Scott Sandstone are distinctive in containing a high proportion of very high pyrope, low grossular types (grossular <10%, pyrope >30%). Low grossular types also dominate the Piper Sandstone garnet assemblages, but pyrope contents are lower, mainly falling in the 20–30% pyrope range (Fig. 4).

Magnetic measurements were performed on the 150–250 μm fraction, which constituted 25–95% of the unfractionated sample mass. The $\%IRM_{0.3-1\ T}$, which is an indicator of the amount of haematite (or goethite) is on average 14%, indicating that a mostly magnetite-like mineral dominates the magnetic properties, with a much smaller contribution from haematite (or goethite). The SCF values were greater than 0.4 for only three parameters ($\%IRM_{20-50\ mT}$, χ_{ARM}/SIRM and SIRM), with $\log_{10}$ [SIRM] used in the cluster statistics (Table 3). The cluster analysis indicates that there are two main clusters, a PB-cluster, which shows a hierarchical subdivision into

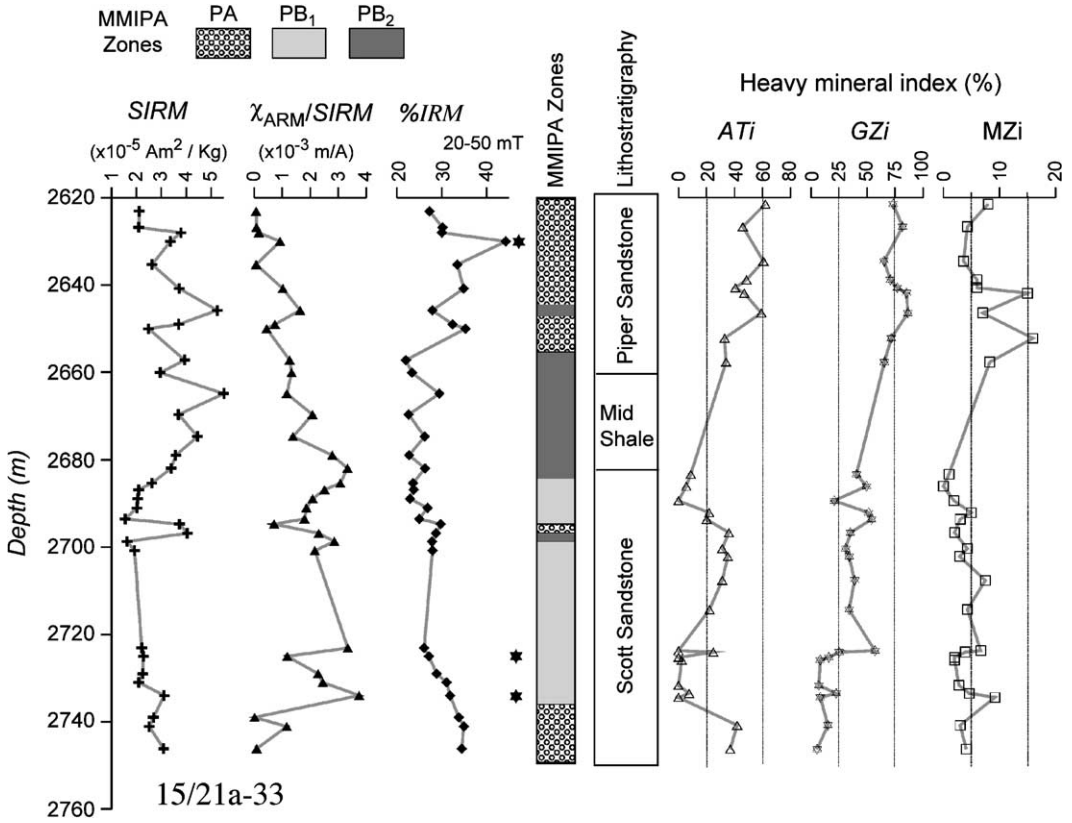

Fig. 3. Down section plot of magnetic and heavy mineral data from the Scott Sandstone and Piper Sandstone formations from well 15/21a-33, along with the MMIPA zonation. Those sample levels marked with * are potentially discordant points in relationship to adjacent data points, and are labeled as such in Fig. 5.

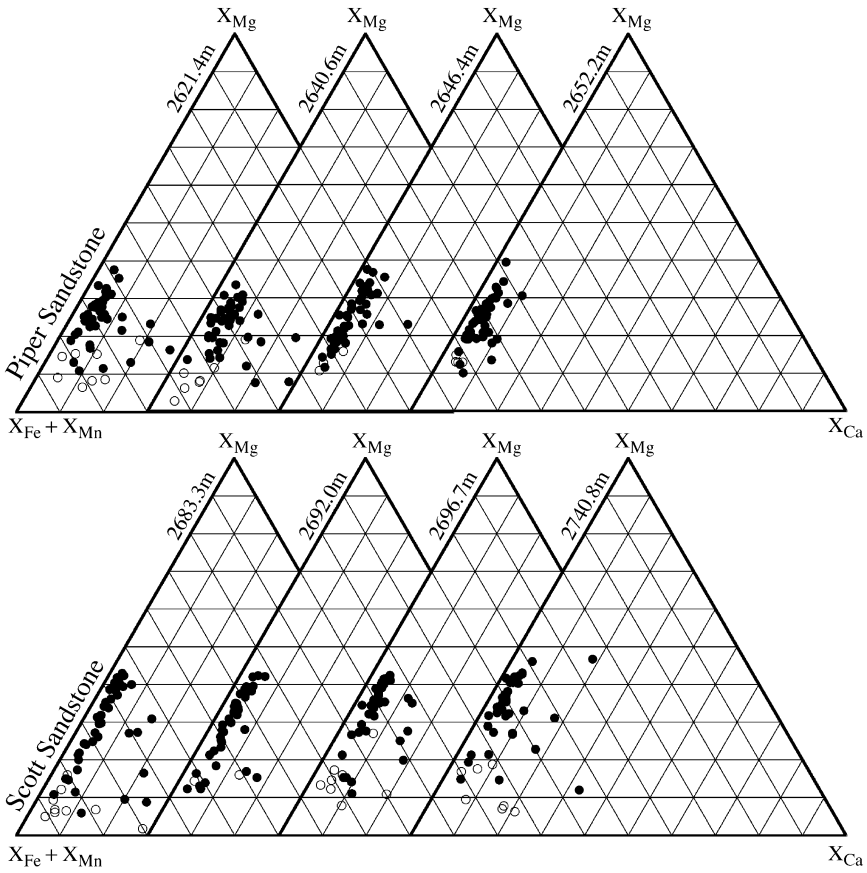

Fig. 4. Garnet geochemistry data for the Scott and Piper Sandstones in well 15/21a-33. X_{Fe}, X_{Mg}, X_{Ca}, X_{Mn}=molecular values of Fe, Mg, Ca and Mn respectively, calculated on the basis of 24 oxygens, and normalised to total Fe+Mg+Ca+Mn, as recommended by Droop and Harte (1995). All Fe calculated as Fe^{2+}. From Morton et al. (2004). ●—X_{Mn}<5%. ○—X_{Mn}>5%.

two subclusters, PB_1 and PB_2 (Figs. 3 and 5). The PA-cluster is mainly distinct from the PB cluster in that it shows elevated values of $\%IRM_{20-50\ mT}$ and low values of χ_{ARM}/SIRM (Table 3). The PA-cluster also has $\%IRM_{0-20\ mT}$, some 10% lower on average than the PB-cluster values at about 33%. This suggests the major difference between the PA and PB-cluster is due to a relatively larger amount of fine-grained, single-domain magnetite-like grains in the PB cluster. Comparison with the synthetic magnetite data of Maher (1988) would suggest the PB cluster has magnetite on average with a magnetic grain size of about 0.02 μm, whereas the PA cluster is larger at about 0.1 μm. The distinction between the two subclusters of PB is mainly on the basis of the SIRM, which shows larger values of SIRM in subcluster PB_2 (Table 3). This high magnetic mineral abundance in PB_2 is also expressed in the mean χ_{ARM} value and χ_{lf} which is the largest of the three clusters (Table 3).

The MDS representation of the data mostly accords with the sample subdivision according to the hierarchical cluster analysis, except for samples at 2725 m and 2734 m depth (Fig. 5). Hence, there is reason to not take the HCA classification of the samples at 2725 and 2734 m at face value, and these samples are considered most similar to the PB_1 subcluster. This also makes more stratigraphic sense, since PB_1 subcluster members are stratigraphically adjacent to both these samples (Figs. 3 and 5).

The stratigraphic distribution of the PB_1-cluster overlaps with the Scott Sandstone and those samples

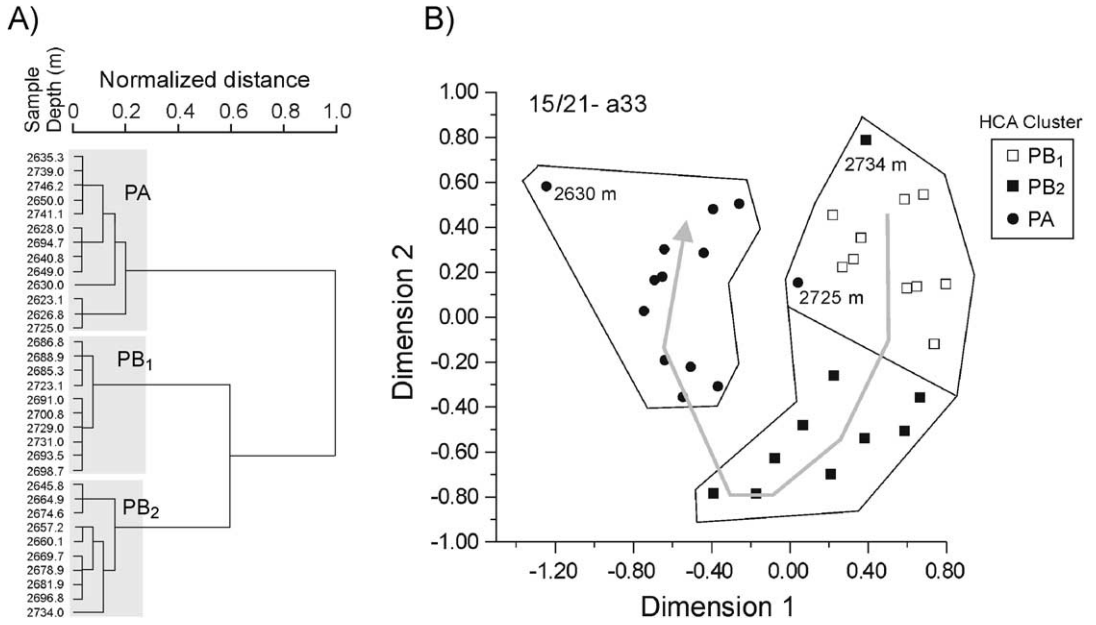

Fig. 5. Cluster analysis data from the Scott and Piper Sandstones in Well 15/21a-33. (A) Dendrogram from the hierarchical cluster analysis, showing the subdivision of sample levels (grey boxes), into the three interpreted MMI source characteristics. The horizontal distance scale on the dendrogram is normalized to the maximum value of the agglomeration coefficient, which occurs when all samples are agglomerated into a single cluster. (B) Multidimensional scaling plot, along with the cluster assignment based on the hierarchical cluster analysis. The grey arrow shows the general up-well evolution of the MMI properties, starting from about 2735 m in the well.

with low ATi values; although the lowest 10 m of the Scott Sandstone have more MMI similarity to the Piper Sandstone (Fig. 3). Those samples belonging to the PB_1-cluster have a comparable stratigraphic range to those with ATi <20% and GZi >10% and <50% (Fig. 3). The thin sandstones sampled in the mid-shale and the basal sample in the Piper Sandstone show a grouping transitional to the Scott Sandstone proper.

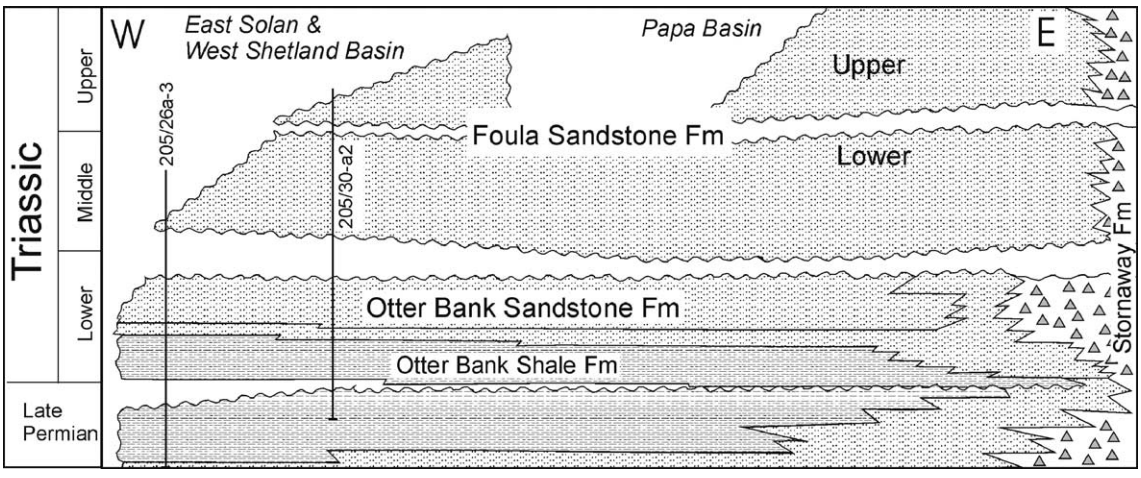

Fig. 6. Summary stratigraphy for the East Solan Basin, simplified from Swiecicki et al. (1995).

This is also evident from the MDS plot, which shows an upwards-directed stratigraphic evolution starting at about 2735 m from PB_1 to PB_2 to PA cluster groupings (Fig. 5). The largest value of MDS dimension 2 in the PA-cluster is from the uppermost samples from the well (Figs. 3 and 5). This upwards change is directly related to the progressive decline in the magnitude of the χ_{ARM}/SIRM (Fig. 3).

Below 2735 m, the Scott Sandstone in the well shows Piper Sandstone affinities, with PA-cluster membership and ATi values greater than 40%. The high ATi value suggests less extensive weathering than stratigraphically higher in the Scott Sandstone succession. The higher ATi value could mean less prolonged alluvial storage, although less humid climatic conditions could provide an explanation. The garnet data and other heavy mineral parameters indicate no substantial difference in the source rock mineralogy. The change in the MMI grouping in the Scott Sandstone below 2740 m may be in part related to an additional 'Piper-like' sand source, but with low GZi indices.

5.3. Case study 2: Foula Sandstone and Otter Bank Sandstone formations

The Triassic of the Strathmore area, west of Shetland, has been subdivided into three formations, the Foula Sandstone Formation, the underlying Otter Bank Sandstone Formation, and the basal Otter Bank Shale Formation (Swiecicki et al., 1995; Fig. 6). On the basis of palynological assemblages, the Otter Bank Shale Formation is believed to be Griesbachian (earliest Triassic) in age (Fig. 6). The age of the Otter Bank Sandstone is less well constrained, but is perhaps lower Triassic to Anisian, and the Foula Sandstone is believed to range from Ladinian to Carnian, or possibly Norian, in age (Swiecicki et al.,

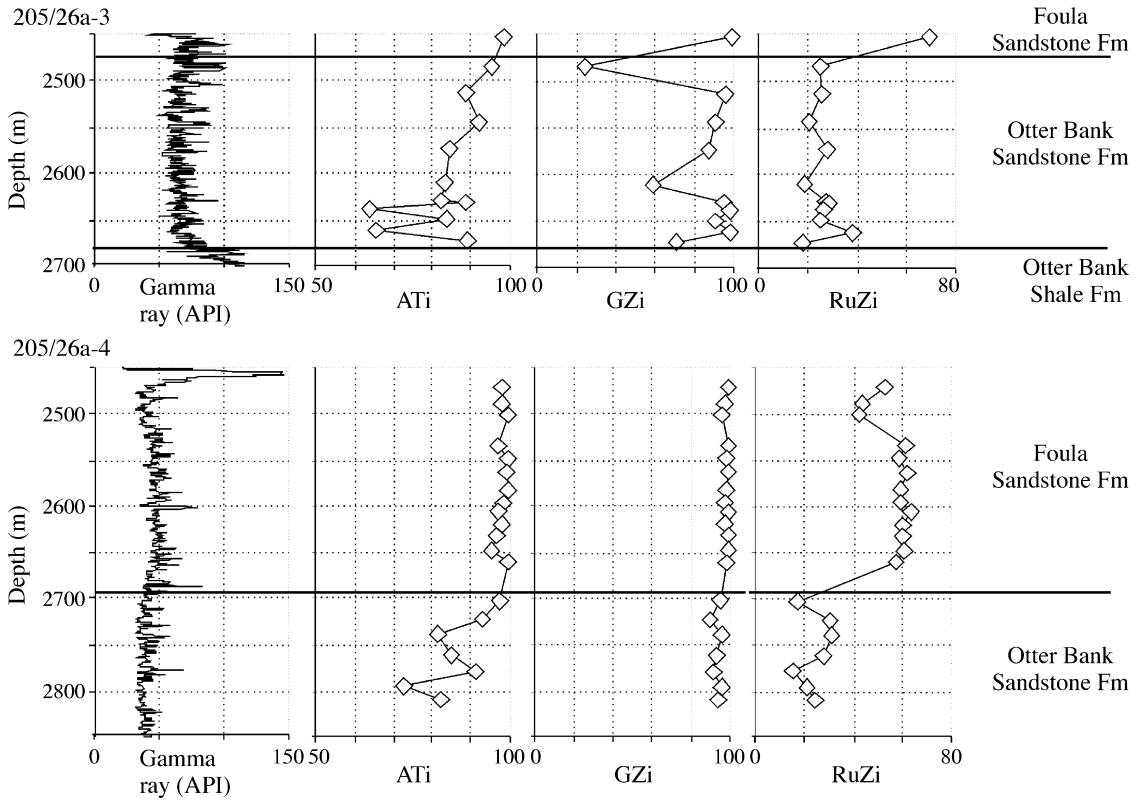

Fig. 7. Downhole profiles of heavy mineral data from the Foula and Otter Bank Formations in 205/26a-3 and the adjacent well 205/26a-4, from Morton et al. (in press(a)). Gamma ray logs follow American Petroleum Institute (API) standard.

1995). The Otter Bank Shale was deposited in a playa lake to coastal/alluvial plain environments, whereas the Otter Bank Sandstone and Foula Sandstones represent a variety of fluvial environments.

Core from well 205/26a-3 cover the basal part of the Foula Sandstone Formation (2450.6–2481.7 m), with the bulk of the core (2481.7–2679.8 m) taken in the Otter Bank Sandstone Formation. Sandstones from the Foula Sandstone Fm are feldspar-poor, mica-poor, poorly sorted sub-lithic arenites. Otter Bank Fm sandstones are mostly feldspar-rich, with subordinate lithic-rich varieties (Herries et al., 1999). These show an overall upwards decrease in feldspar content, with a lower unit (2622.2–2679.8 m) containing poor or moderately sorted, feldspar-rich (~25%) arenite, and an upper unit (2481.7–2622.2 m) with generally lower feldspar contents. The Foula and Otter Bank Sandstones are very similar in grain size with the mean grain size for sandstone specimens ranging from 120 to 300 μm. The samples from the Foula Sandstone tend to be white to very pale grey, whereas the Otter Bank Sandstones tend to be pale to dark greyish brown. The original red body-colour of these sandstones has probably been bleached by acidic ground waters during deep burial (Herries et al., 1999).

5.3.1. Heavy mineral data

Heavy mineral data from 205/26a-3 and the adjacent well 205/26a-4 indicate a primary differ-

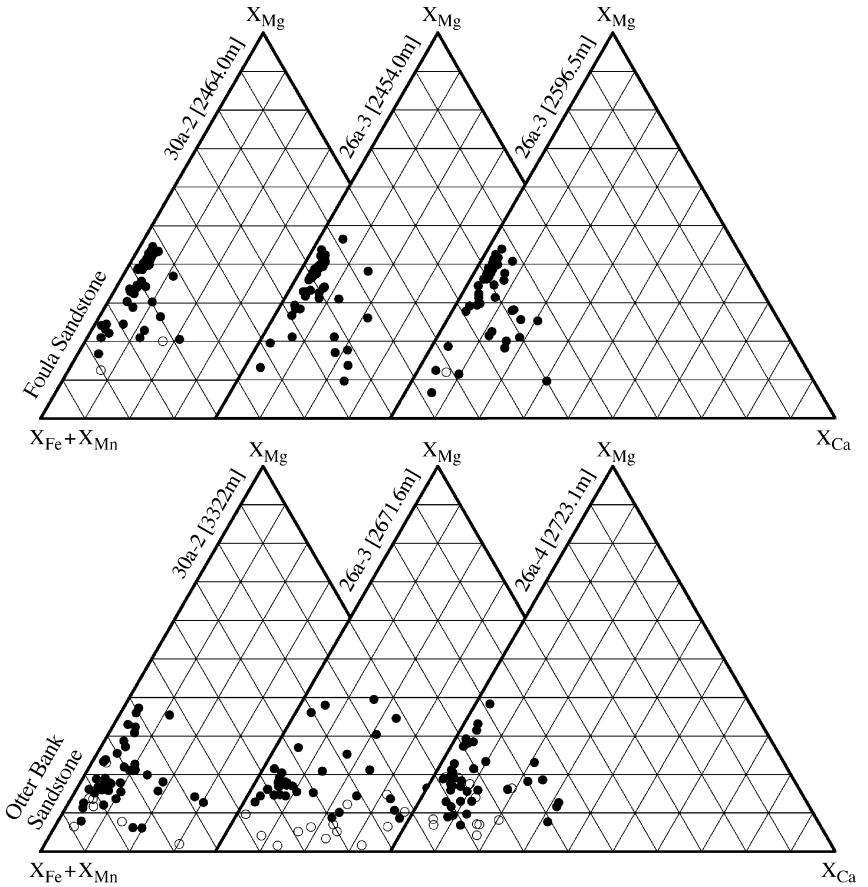

Fig. 8. Garnet compositions in selected samples from Foula Sandstone and Otter Bank Sandstone formations in the Strathmore Field (from Morton et al., in press(a)). X_{Fe}, X_{Mg}, X_{Ca}, X_{Mn}=molecular values of Fe, Mg, Ca and Mn, respectively, calculated on the basis of 24 oxygens, and normalised to total Fe+Mg+Ca+Mn, as recommended by Droop and Harte (1995). All Fe calculated as Fe^{2+}. ●—X_{Mn}<5%. ○—X_{Mn}>5%. Wells (all from sector 205) and sample depths are indicated for each ternary diagram.

ence in provenance between the Foula Sandstone and the Otter Bank Sandstone (Morton et al., in press(a)). The Foula Sandstone has very high RuZi, GZi and ATi values, and has a garnet assemblage dominated by high pyrope, low grossular types (Figs. 7 and 8). By contrast, the Otter Bank Sandstones have consistently low RuZi values, show some variation in GZi and ATi (Fig. 7), and have garnet assemblages dominated by low pyrope types with variable grossular contents (Fig. 8). The marked variations within the Otter Bank Sandstone indicate the provenance of this unit is relatively heterogeneous.

5.3.2. Magnetic inclusion data

The broader spread of grain sizes and larger sample mass has allowed the magnetic measurements to be applied to all three size fractions. However, the data from the different grain size fractions are variable in response, the details of which are considered in Section 6. The coarser grain size fractions (150–250 and 250–500 μm) show the most sensitive response to changing sources, with the finer fraction (38–150 μm) indicating a more noisy record. Hence, the finer fraction was not used in the MMI interpretation. The definitive cluster analysis was performed using both the 150–250 and 250–500 μm fractions, which together represent on average some 85% of the mass of the clastic fraction.

In total, there were 29 MMI parameters (out of 34 possible) from these two fractions which possessed an SCF >0.4. Many of these duplicated the same kind of stratigraphic variation, which was not helpful to the cluster analysis (Lees, 1999). Consequently, parameters were flagged for potential exclusion on the basis of the between-variables, Pearson cross-correlation coefficient (r). Those variables with the lowest SCF were excluded when the r-value exceeded $|0.8|$. This exclusion process for the 150–250 and 250–500 μm fractions leads to five parameters being retained for each fraction (Table 4).

The MMI provenance differences are characterised using the two separate grain size fractions together, so that each stratigraphic level had effectively 10 parameters for the cluster analysis. The HCA and MDS indicate separation into three main clusters, the Foula Sandstone (cluster F) and two in the Otter Bank Sandstone, with these clusters designated O_3 and O_2+O_1 (Figs. 9 and 10B). The cluster naming system is based on data discussed in Section 6. The cluster O_1+O_2, can be subdivided into three subclusters (O_1, O_{2a}, O_{2b}), apparent in the dendrogram (Fig. 10A). Of

Table 4
Summary of magnetic properties for the MMI provenance clusters for samples from the Otter Bank and Foula sandstones in Well 205/26a-3, for sand fractions 180–250 and 250–500 μm

MMI cluster	N	χ_{HIRM}[a] $\times10^{-10}$ m^3/kg	χ_{ARM}[a] $\times10^{-8}$ m^3/kg	S-ratio	$\%IRM_{50–100\ mT}/\%IRM_{0.1–0.3\ T}$	χ_{ARM}/SIRM $\times10^{-3}$ m/A	$\%IRM_{0.3–1\ T}$
Fraction 150–250 μm							
F	5	0.273	25.5	1.55	2.59	1.47	8.9
O_1	8	0.144	11.11	1.38	1.80	1.74	13.2
O_2+O_3	18	0.108	6.09	1.34	1.50	1.20	12.0
SCF		0.54	0.79	0.78	0.75	0.51	0.36
		χ_{ARM}[a] $\times10^{-8}$ m^3/kg	$\%IRM_{20–50\ mT}$	$\%IRM_{0.1–0.3\ T}$	$\%IRM_{20–50\ mT}/\%IRM_{50–100\ mT}$	χ_{ARM}/SIRM $\times10^{-3}$ m/A	$\%IRM_{0.3–1\ T}$
Fraction 250–500 μm							
F	3	21.10	33.74	14.42	1.04	1.34	12.3
O_1	8	10.18	27.75	18.50	0.91	1.52	12.6
O_2	8	6.54	28.12	18.96	0.94	1.22	14.4
O_3	9	3.73	27.27	22.23	0.88	1.12	15.8
SCF		0.61	0.69	0.76	0.72	0.77	0.53

[a] Indicates a log mean was determined. SCF is the stratal consistency function. N=number of samples.

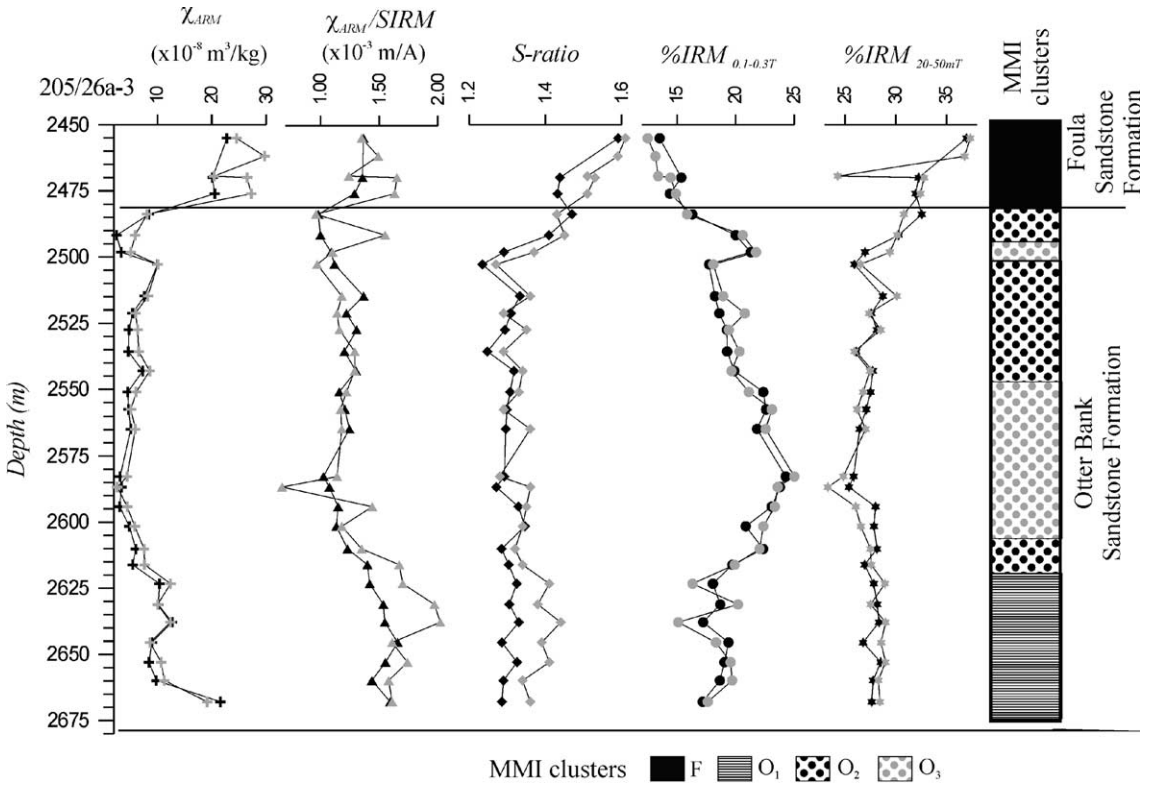

Fig. 9. Plot of selected magnetic parameters from well 205/26a-3. The black filled symbols are the data for the 250–500-μm fraction and the gray filled symbols for the 125–250-μm sand fraction.

these, only the O1 subcluster is stable with grain size change (Fig. 11A,B).

The F-cluster is characterised by larger MMI abundance parameters (SIRM, χ_{ARM} and χ_{HIRM}), indicating increased abundance of magnetite compared to the Otter Bank Sandstone (Table 4). In contrast, the O_3 cluster is characterised by the lowest proportions of ferrimagnetic material (SIRM, χ_{ARM} and χ_{HIRM}). The samples belonging to the O_3 cluster may contain rather coarser-grained ferrimagnets (i.e. probably magnetite) than in other units, indicated by the lowest mean χ_{ARM}/SIRM, although the larger values of the %IRM $_{0.1–0.3\ T}$ (and %IRM $_{50–100\ mT}$) may indicate it is rich in elongate magnetite. Group O_3 is higher in haematite compared to other units (e.g. high %IRM$_{0.3–1\ T}$; Table 4). The O_1 cluster is characterised by moderate abundances of magnetite and haematite, shown by SIRM, χ_{ARM} and χ_{HIRM}. It also has a distinctively large χ_{ARM}/SIRM corresponding to larger amounts of ultrafine magnetite.

The clusters fall into distinct stratigraphic intervals in the well (Fig. 9). The O_1 cluster is confined to the lower parts of the Otter Bank Sandstone, below 2616 m, corresponding to an interval with variable but often low (<80) ATi values (Fig. 7). Most of this interval also corresponds to the lower feldspar-rich part of the Otter Bank Sandstone. The O_2+O_3 group is confined to the upper part of the Otter Bank Sandstone, and the F-cluster to the Foula Sandstone (Fig. 9b). The O_2 subcluster is largely restricted to the uppermost part of the Otter Bank Formation, whereas the O_3 subcluster is restricted to the 2545–2605 m interval (Fig. 9b). Three sample levels (2483.8, 2491.7 and 2502.8 m) assigned to the O_2 subcluster do not fall into the tight cluster associated with each of the main sample groupings on the MDS diagram (Fig. 10B). This indicates these three samples have MMI characteristics with marginal similarity to the O_2 cluster to which they are assigned. These three marginal samples form three of the four

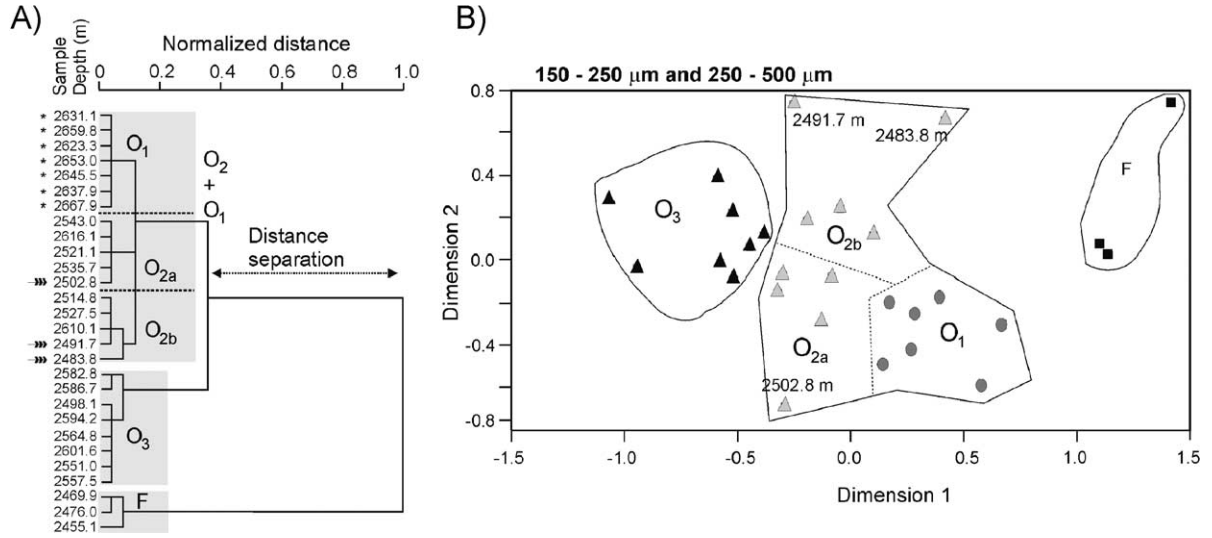

Fig. 10. Cluster analysis of the Foula and Otter Bank sandstones in well 205/26a-3, using the combined 150–250- and 250–500-μm fractions. (A) Dendrogram from the hierarchical cluster analysis, showing the subdivision of sample levels (grey boxes), into the three main interpreted MMI sources F, O_3, O_2+O_1. The agglomerated O_1+O_2 cluster is subdivided into three subgroups (O1, O_{2a}, O_{2b}), the boundaries of which are indicated by the dotted lines. The sample levels flagged with * are those which are assigned to the O_1 cluster in the cluster analysis of the 250–500-μm fraction (Fig. 11A). Those sample levels flagged with an arrow are the outlying samples indicated in (B). The horizontal distance scale on the dendrogram is normalized to the maximum value of the agglomeration coefficient. The distance separation between the stages at which the F and O_2+O_1+O_3 clusters join in the dendrogram is shown. (B) Multidimensional scaling plot of the samples and the main MMI clusters based on the dendrogram from the hierarchical cluster analysis, shown in (A). Note the large central cluster is subdivided into three subclusters (O_1, O_{2a} and O_{2b}).

stratigraphic levels in the Otter Bank Sandstone immediately below the Foula Sandstone (Fig. 10A), providing an indication for the hypothesis of an ill-defined, divergent MMI source restricted to the uppermost part of the Otter Bank Sandstone Formation. ATi values in excess of 95 at the top of the Otter Bank Sandstone Fm also show characteristics transitional to the high ATi values within the Foula Sandstone (Fig. 7), giving some additional support for this hypothesis.

The cluster analysis also allows the determination of the distinctiveness of the major cluster groups. Two measures of this distinctiveness can be gained from the data. Firstly, the distances on the MDS plot between the clusters. The closeness of the O_1, O_2 and O_3 clusters implies the Otter Bank Sandstone clusters are most distinct from the Foula Sandstone F-cluster (Fig. 10B), as is also suggested by the heavy mineral data. Secondly, a measure of the MMI distinctiveness can be gauged by the 'distance separation' from the HCA dendrogram, which measures the normalized distance in the agglomeration schedule at which the sample data merge into clusters in the HCA (Fig. 10A). This distance separation suggests the F cluster is most distinct from the O-clusters, with a distance separation of 0.64, as also suggested by the MDS plot (Figs. 10 and 12B). The O_3 cluster is the most distinctive unit within the Otter Bank Sandstone, with a distance separation of 0.24 (Fig. 12B) from the merged O_1+O_2 clusters (Figs. 10A and 12B). The subcluster divisions within the O_1+O_2 cluster are relatively similar, in that they merge at a similar low level in the agglomeration schedule (Fig. 10A).

6. Comparison between grain size fractions

The MMI provenance technique could potentially be applied to many sediment grain size fractions. Hence, it is important to ascertain, (a) which fraction is likely to be the most powerful for discriminating provenance differences in any particular study, and (b) how the MMI properties might change with host grain size. Currently, both these factors are poorly under-

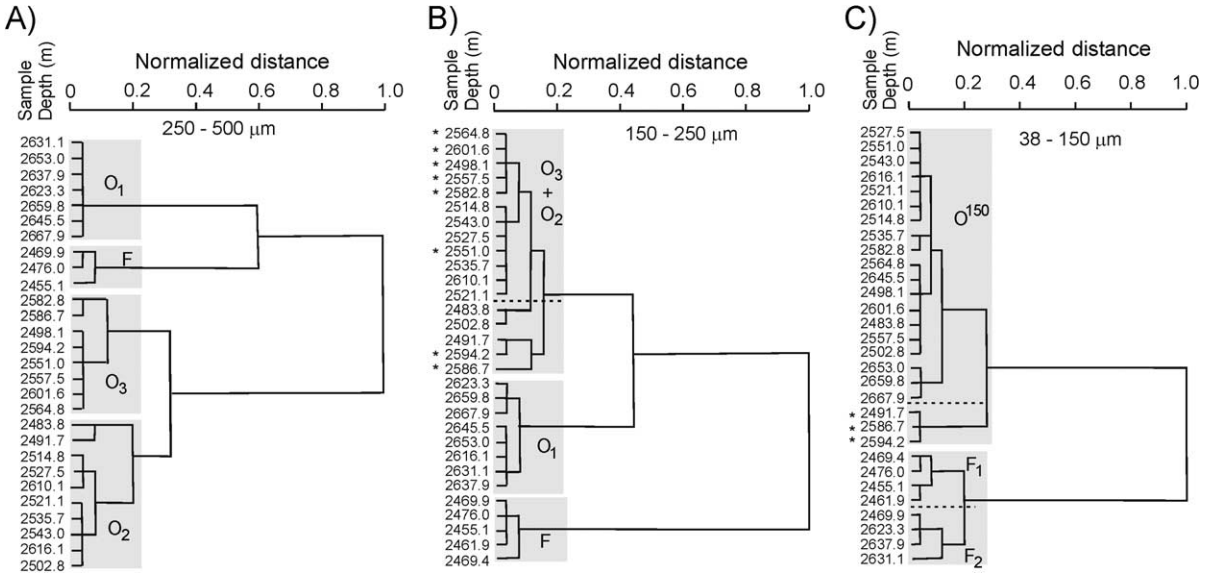

Fig. 11. Hierarchical cluster analysis of the Foula and Otter Bank sandstones in well 205/26a-3, using the (A) 250–500 μm, (B) 150–250 μm and (C) 38–150 μm grain size fractions. (A) The most distinct separation of the four MMI clusters F, O_1, O_2, O_3 occurs for the 250–500-μm fraction, evident by the large separation distances at cluster merging, with the O_2 and O_3 clusters having the smallest separation distance (0.12) at merging. (B) The O_1 cluster and F clusters are stable using the 150–250-μm fraction, whereas the O3 and O2 clusters merge. Those sample levels flagged with * correspond to the O_3 cluster in (A). (C) The 38–150-μm fraction shows the breakdown of clusters evident in (A) and (B) into two main clusters, with the F_1 cluster restricted to the Foula Sandstone (see Fig. 12).

stood. Examination of the provenance discrimination behaviour of the three grain size fractions from the Foula and Otter Bank Sandstones provides a start in this understanding.

6.1. Which host grain size is the most powerful for MMI provenance discrimination?

Although different sediment sources may have different MMI properties, there is no guarantee that a set of magnetic measurements will allow the discrimination of these sources. Factors which perturb this are, (a) the sensitivity of the measurements to the differences in the MMI properties, (b) the added noise due to the measurement and subsampling procedures, (c) the natural variability in the MMI behaviour from a single source due to environmental factors such as hydraulic sorting and weathering, and (d) local host changes due to diagenesis (i.e., stratigraphic sampling effects). Hence, the 'noise' in the system has a strong effect on the ability of the MMI (or any other technique) to detect differences in provenance.

A measure of the strength of the provenance sensitivity can be gauged by how much the MMI properties rise above this noise in the system. The SCF value of a magnetic variable is an approximation of the stratigraphic noise in the system, since it is a measure of the stratigraphic consistency of adjacent magnetic measurements. Consequently, the overall magnitudes of the SCF of all variables can be used to gauge the sensitivity of provenance detection to changes in host grain size. Of the 17 magnetic parameters calculated for each of the three grain-size fractions in the Foula and Otter Bank case study 10, 12 and 17 variables exceed an SCF value of 0.4 in the 38–150, 150–250 and 250–500 μm fractions, respectively. In addition 2, 9, and 11 variables exceed an SCF value of 0.6 in the 38–150, 150–250 and 250–500 μm fractions respectively. This suggests that the coarser fractions are lowest in noise, because these contain the highest number with large SCF values. Hence for this study the 250–500 μm fraction is some 1.7 to 5.5 more sensitive than the 38–150 μm and some 1.2 to 1.4 times more sensitive than the 150–250 μm fraction in potentially detecting changes in

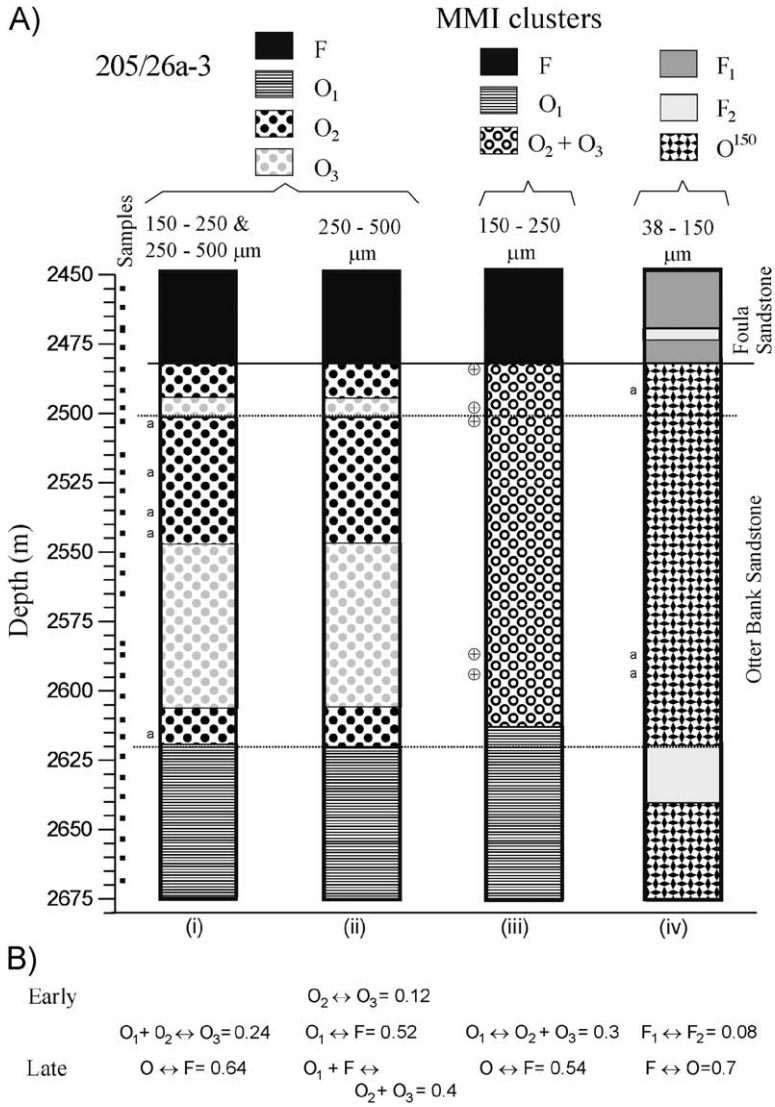

Fig. 12. (A) Magnetic mineral inclusion zonation of the Otter Bank and Foula Sandstones, well 205/26a-3. The stratigraphic distribution of the HCA cluster groupings is shown for four separate analyses using the three grain size fractions. HCA dendrograms for these four cases are shown in Figs. 10A and 11. Column (i) 'a'=those sampling horizons assigned to the O_{2a} cluster. Column (iii), ⊕=position of samples belonging to lower subcluster in O_3+O_2 cluster in Fig. 11B. Column (iv) 'a'=position of samples belonging to subcluster O^{150a}. (B) Data displaying the distance separation of the HCA clusters, and their stages of merging on the HCA dendrograms shown in Figs. 10 and 11. The value after the = is the distance separation, and before this in each cell, are the clusters that are involved at this stage. Clusters which merge early and late in the dendrogram are indicated by their placement in the columns. + indicates agglomerated clusters or subclusters from an earlier stage in the dendrograms.

provenance. Alekseeva and Hounslow (2004) have come to a similar conclusion, using a fluvial–glacial data set from the Russian Pleistocene.

The effect of changes in host grain size upon the stratal classification based on the HCA has been examined for the three host grain size fractions. The HCA was repeated separately for each grain size fraction, and their resulting HCA classifications are show in Figs. 11 and 12. From this, it is apparent that the classifications are very similar using either the 150–250 or 250–500 µm fractions. In both these cases, the O_1 and F clusters contain the same samples,

with any differences largely related to the subcluster membership of the remaining samples (Fig. 11A,B). However, the later stages of the cluster joining are swapped around, such that the cluster O_1 is most similar to the F cluster in the 250–500 μm fraction and O_1 most similar to the O_2+O_3 cluster in the 150–250 μm fraction. The strongest separation of the four HCA clusters also occurs for the 250–500 μm fraction. Both this, and the previous noise sensitivity analysis, implies that the 250–500 μm fraction provides the most robust provenance discrimination. This fraction is therefore used to provide the cluster naming conventions in Figs. 10, 11 and 12. The stratigraphic distribution of HCA clusters for the 250–500 μm fraction is most similar to the HCA using the combined 150–250 and 250–500 μm fractions (Fig. 12A). This is due to the HCA preferentially weighting those parameters from the 250–500 μm fraction due to their less 'noisy' characteristics, reducing the sensitivity of the clustering to the more noisy parameters from the 150–250 μm fraction (cf. Milligan, 1980).

The stratigraphic grouping of the O_3+O_2 clusters breaks down for the 150–250 μm fraction, so that realistically only the interval below 2610 m can be separated from the upper part of the Otter Bank Sandstone in well 205/26a-3 (Fig. 12A). For the 38–150 μm fraction, the previous groupings break down, and the HCA indicates a new larger F cluster and a new Otter Bank Sandstone cluster (called O^{150}). The F-cluster is divisible into two subclusters, with the F-cluster not now restricted to the Foula Sandstone. However, even though the 38–150-μm fraction is more noisy (based on the above SCF argument), this fraction still retains the subdivision of the Otter Bank Sandstone into a twofold unit, with below 2621 m being an F_2 and O^{150} dominated unit, and above this an O^{150} cluster dominated unit.

6.2. Magnetic property changes with grain size

For each sample, all magnetic parameters in each of the grain size fractions were normalised to those in the 150–250-μm fraction, allowing comparison of the

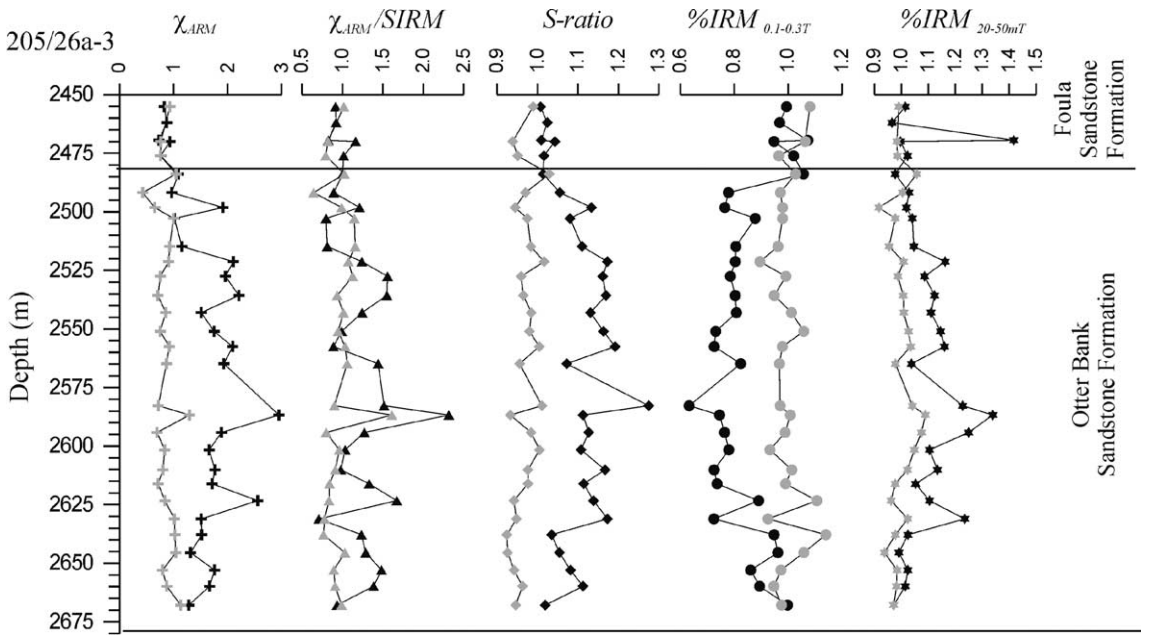

Fig. 13. Differences in magnetic properties between the three grain-size fractions, using the selected magnetic parameters from the Foula/Otter Bank Sandstone case study, well 205/26a-3. In each case, the magnetic properties of each sand fraction sample have been divided by the magnetic properties of the 125–250 μm fraction. Hence, if the fraction has a larger value of this parameter, it will have a value exceeding 1, and if small a value less than 1. Black filled symbols for the 38–125 μm sand fraction, gray filled symbols for the 250–500 μm fraction. Overall, the 250–500 and 125–250 μm fractions have the most similar magnetic properties.

magnitude of the magnetic parameters. In general terms, there is a distinct difference in magnetic response across the grain size fractions between the Foula Sandstone and the Otter Bank Sandstone. The Foula Sandstone is noticeably more consistent between grain size fractions than the Otter Bank Sandstone, which shows distinct inter-fraction differences (Fig. 13). The changes shown by the Otter Bank Sandstone imply that the 38–150 μm fraction is consistently enriched in magnetically soft (i.e. larger) magnetite particles and consistently depleted in haematite (or goethite) compared to other fractions. By contrast, fractions coarser than 150 μm are relatively consistent over all magnetic parameters. This shows, that in the case of well 205/26a-3, the 150–500 μm fractions have a relatively similar inclusion (and host?) mineralogy, which is the reason for the consistency between the stratal classifications of these two size fractions.

One reason for the different response of the <150-μm fraction is probably due to its greater content of heavy minerals (Morton and Hallsworth, 1999). Other studies of the magnetic properties of sediments indicate that heavy minerals can contain a significant number of magnetic inclusions (Hounslow et al., 1995; Hounslow and Maher, 1996), which will bias the finer grain fractions to having larger magnetic abundance parameters such as χ_{ARM} (Fig. 12). Another possibility is that the <150-μm fraction may contain detrital Fe-rich chromites, since these can sometimes be significant contributors to the magnetic signal (Hounslow, 1996), but are resistant to the dissolution treatment, which isolates the inclusions. However, heavy mineral analysis indicates that chrome spinel is scarce in both the Foula and Otter Bank Sandstones.

7. Conclusions

Fe-oxide inclusions are for the most part widely dispersed in the light mineral fraction of sediments. Hence, the sensitivity of the MMI technique is strongly biased towards the framework components of clastic sediments. The fact that there is a good correspondence between the major MMI characteristics and the heavy mineral data in the two case studies indicates the close linkage to sediment provenance in both the light and heavy mineral fractions.

The origin of the Fe-oxide inclusions is intimately related to the origin of the host particles and hence the magnetic properties of the inclusions are probably controlled by the local petrogenetic conditions forming the host, along with the stress and heating history of the source rock. This is seen in the distinct separation of primary sources for recent sediments, which form sample Set A of this study.

The Fe-oxides in the host mineral are largely isolated from pore fluids that are aggressive to discrete Fe-oxides, and therefore will be preserved even during deep burial, provided the host is also preserved. The dissolution of unstable minerals during diagenesis may have an impact upon the MMI signal, although other provenance techniques may also be similarly affected. Resetting of the MMI signal within quartz and feldspar grains may not occur until these grains recrystallise during metamorphism. Consequently below this metamorphic level, there is good potential for inheritance of MMI signals from erosion of sedimentary and low-grade metamorphic rocks.

Provenance discrimination is based on utilising a specific host particle size range, which may be changed to suit the sediment grain size. The coarser end of the grain size distribution for any particular sediment is likely to provide the fraction most sensitive for MMI characterisation. The extent to which this is the case for all successions is uncertain. However, the finest clastic fraction still retains the imprint of provenance changes in the MMI properties, albeit with a lower sensitivity than the coarser fractions.

The magnetic characterisation methods are inexpensive, quick and easily adapted to rigorous statistical analysis. The statistical analysis is an important part of the MMI approach because the sets of magnetic measurements ‘over-describe’ the MMI properties. Statistical techniques are therefore necessary to exclude redundant or noisy parameters, leaving a sensitive subset. This is especially important because there is currently no other objective way to determine information about which subset of magnetic parameters to use in any particular analysis. The statistical techniques are also adaptable, because given suitable end-member sediment sources; they can be used to determine sediment loads and end-member mixing relationships (Caitcheon, 1998; Lees, 1999).

The nature and origin of the inclusions in host silicates (especially quartz) within sediments have not been described in the literature in any detail. In the longer term, better understanding of the origin, controls and magnetic characteristics of Fe-oxide inclusions will lead to better interpretation of provenance signatures provided by the magnetic inclusions, although currently this conceptual linkage is weak.

Acknowledgements

All subsurface samples described were kindly made available by Amerada Hess, or the DTI core store, Edinburgh. Cassandra Woods measured the magnetic samples from 15/21a-33, and Rob Hawkins the magnetic samples from 205/26a-3. Maria Mange and an anonymous reviewer improved the manuscript.

References

Alekseeva, V.A., Hounslow, M.W., 2004. Clastic sediment source characterisation using discrete and included magnetic particles-their relationship to conventional petrographic methods in early Pleistocene fluvial-glacial sediments, Upper Don River Basin (Russia). Phys. Chem. Earth 29, 961–971.

Armbrustmacher, T.J., Banks, N.G., 1974. Clouded plagioclase in metadolorite dykes, southeastern Bighorn Mountains, Wyoming. Am. Mineral. 59, 656–665.

Boote, D.R.D., Gustav, S.H., 1987. Evolving depositional systems within an active rift, Witch Ground Graben, North Sea. In: Brooks, J., Glennie, K.W. (Eds.), Petroleum Geology of North West Europe. Graham and Trotman, London, pp. 819–833.

Brearley, A.J., Champness, P.E., 1986. Magnetite exsolution in almandine garnet. Mineral. Mag. 50, 621–633.

Caitcheon, G.G., 1998. The significance of various sediment magnetic mineral fractions for tracing sediment sources in Killimicat Creek. Catena 32, 131–142.

Canfield, D.E., Berner, R.A., 1987. Dissolution and pyritisation of magnetite in anoxic marine sediments. Geochim. Cosmochim. Acta 51, 645–659.

Canfield, D.E., Raiswell, R., Bottrell, S., 1992. The reactivity of sedimentary iron minerals towards sulfide. Am. J. Sci. 292, 659–683.

Dearing, J.A., 2000. Natural magnetic tracers in fluvial geomorphology. In: Foster, I.D.L. (Ed.), Tracers in Geomorphology. John Wiley and Sons, London, pp. 57–82.

Dekkers, M.J., 1997. Environmental magnetism: an introduction. Geol. Mijnb. 76, 163–182.

Droop, G.T.R., Harte, B., 1995. The effect of Mn on the phase relations of medium-grade pelites: constraints from natural assemblages on petrogenetic grid topology. J. Petrol. 36, 1549–1578.

Dunlop, D.J., Ozdemir, O., 1997. Rock Magnetism: Fundamentals and Frontiers. Cambridge Univ. Press, Cambridge.

Evans, M.E., Heller, F., 2003. Environmental Magnetism: Principles and Applications of Enviromagnetics. Academic Press, London. 382 pp.

Evans, M.E., Wayman, M.L., 1970. An investigation of small magnetic particles by electron microscopy. Earth Planet. Sci. Lett. 9, 365–370.

Folk, R.L., 1974. Petrology of Sedimentary Rocks. Hemphill Publishing, New York.

Fowlkes, E.B., Gnanadesikan, R., Kettenring, J.R., 1988. Variable selection in clustering. J. Classif. 5, 205–228.

Frost, B.R., 1991a. Stability of oxide minerals in metamorphic rocks. In: Lindsley, D.H. (Ed.), Oxide Minerals, Reviews in Mineralogy, vol. 25. Mineralogical Soc. Amer., pp. 467–487.

Frost, B.R., 1991b. Magnetic petrology: factors that control the occurrence of magnetite in crustal rocks. In: Lindsley, D.H. (Ed.), Oxide Minerals, Reviews in Mineralogy, vol. 25. Mineralogical Soc. Amer., pp. 489–509.

Geissman, J.M., Harlan, S.S., Brearley, A.J., 1988. The physical isolation and identification of carriers of geologically stable remanent magnetisation: palaeomagnetic and rock magnetic microanalysis and electron microscopy. Geophys. Res. Lett. 15, 479–482.

Heider, F., Körner, U., Bitschere, P., 1993. Volcanic ash particles as carriers of remanent magnetisation in deep sea sediments from the Kerguelan Plateau. Earth Planet. Sci. Lett. 118, 121–134.

Herries, R., Poddubiuk, R., Wilcockson, P., 1999. Solan, Strathmore and the back basin play, west of Shetland. In: Fleet, A.J., Boldy, S.A.R. (Eds.), Petroleum Geology of Northwest Europe: Proceedings of the 5th Conference. Geological Society, London, pp. 693–712.

Hounslow, M.W., 1996. Ferrimagnetic Cr and Mn spinels in sediments: residual magnetic minerals after diagenetic dissolution. Geophys. Res. Lett. 23, 2823–2826.

Hounslow, M.W., Maher, B.A., 1996. Quantitative extraction and analysis of carriers of magnetisation in sediments. Geophys. J. Int. 124, 57–74.

Hounslow, M.W., Maher, B.A., 1999. Source of the climatic signal recorded by magnetic susceptibility variations in Indian Ocean deep-sea sediments. J. Geophys. Res. 104, 5047–5061.

Hounslow, M.W., Maher, B.A., Thistlewood, L., 1995. Magnetic mineralogy of sandstones from the Lunde Formation (late Triassic), northern North Sea, UK: origin of the palaeomagnetic signal. In: Turner, P., Turner, A. (Eds.), Palaeomagnetic Applications in Hydrocarbon Exploration and Production, Spec. Pub.-Geol. Soc. London, vol. 98, pp. 119–148.

Karlin, R., 1990. Magnetite diagenesis in marine sediments from the Oregon continental margin. J. Geophys. Res. 95, 4405–4419.

Lees, J., 1999. Evaluating magnetic parameters for use in source identification, classification and modelling for natural and environmental materials. In: Walden, J., Oldfield, F., Smith, J.P. (Eds.), Environmental Magnetism: A Practical Guide. Quaternary Research Association, Cambridge, pp. 113–138.

Maher, B.A., 1988. Magnetic properties of some synthetic submicron magnetites. Geophys. J. 94, 83–96.

Maher, B.A., Thompson, R., Hounslow, M.W., 1999. Introduction. In: Maher, B.A., Thompson, R. (Eds.), Quaternary Climates, Environments and Magnetism. Cambridge Univ. Press, Cambridge, pp. 1–48.

Manly, B.F.J., 1994. Multivariate Statistical Methods: A Primer, 2nd edition. Chapman and Hall, London.

Martinez-Monasterio, E., Stephens, W.E., Walden, J., Dick, R.W., 2000. Weathering and abrasion of Fe–Ti Oxides during rock degradation and fluvial transport: implications for sedimentary provenance studies. J. Geol. Soc. (Lond.) 157, 601–613.

Milligan, G.W., 1980. An examination of the effects of six types of error perturbation on fifteen clustering algorithms. Psychometrika 45, 325–341.

Minchin, P.R., 1987. An evaluation of the relative robustness of techniques for ecological ordination. Vegetatio 69, 89–107.

Morad, S., Aldahan, A.A., 1986. Alteration of detrital Fe–Ti oxides in sedimentary rocks. Geol. Soc. Amer. Bull. 97, 567–578.

Morgan, G.E., Smith, P.P.K., 1981. Transmission electron microscope and rock magnetic investigations of remanence carriers in a PreCambrian metadolerite. Earth Planet. Sci. Lett. 53, 226–240.

Morton, A.C., 1984. Stability of detrital heavy minerals in Tertiary sandstones from the North Sea Basin. Clay Miner. 19, 287–308.

Morton, A.C., 1985. A new approach to provenance studies: electron microprobe analysis of detrital garnets from Middle Jurassic sandstones of the northern North Sea. Sedimentology 32, 553–566.

Morton, A.C., Hallsworth, C., 1994. Identifying provenance-specific features of detrital heavy mineral assemblages in sandstones. Sediment. Geol. 90, 241–256.

Morton, A.C., Hallsworth, C.R., 1999. Processes controlling the composition of heavy mineral assemblages in sandstones. Sediment. Geol. 124, 3–29.

Morton, A.C., Herries, R., Fanning, C.M., in press(a). Correlation of Triassic sandstones in the Strathmore Field, west of Shetland, using heavy mineral provenance signatures. In: Mange, M.A, Wright, D. (Eds.) Heavy Minerals in use. Developments in Sedimentology.

Morton, A.C., Hallsworth, C.R., Chalton, B., 2004. Garnet compositions in Scottish and Norwegian basement terrains: a framework for interpretation of North Sea sandstone provenance. Marine and Petroleum Geology. 21, 393–410.

Moseley, D., 1984. Symplectic exsolution in olivine. Am. Mineral. 69, 139–153.

O'Driscoll, D., Hindle, A.D., Long, D.C., 1990. The structural controls on Upper Jurassic and Lower Cretaceous reservoir sands in the Witch Ground graben, UK North Sea. In: Hardman, R.P.F., Brooks, J. (Eds.), Tectonic Events Responsible for Britain's Oil and Gas Reserves, Spec. Pub.-Geol. Soc. Lond., vol. 55, pp. 299–323.

Oldfield, F., 1991. Environmental magnetism—a personal perspective. Quat. Sci. Rev. 10, 73–85.

Oldfield, F., Maher, B., Donoghue, J., Pierce, J., 1985. Particle-size related mineral magnetic source-sediment linkages in the Rhode River catchment, Maryland, USA. J. Geol. Soc. (Lond.) 142, 1035–1046.

Otofuji, Y.I., Uno, K., Higashi, T., Ichikawa, T., Ueno, T., Mishima, T., Matsuda, T., 2000. Secondary remanent magnetisation carried by magnetite inclusions in silicates: a comparative study of unremagnetized and demagnetized granites. Earth Planet. Sci. Lett. 180, 271–285.

Parker, R.H., 1991. The Ivanhoe and Rob Roy Fields, block 15/21a, b, UK North Sea. In: Abbots, I.L. (Ed.), UK North Sea UK Oil and Gas Fields: 25 Years Commemorative Volume, Memoir, vol. 14. Geol. Soc., London, pp. 3318–3331.

Pentecost, A., 1999. Analysing Environmental Data. Longman, Harlow.

Reynolds, R.L., Hudson, M.R., Fishman, N.S., Campbell, J.A., 1985. Palaeomagnetic and petrologic evidence bearing on the age and origin of uranium deposits in the Permian Cutler Formation, Lisbon Valley, Utah. Geol. Soc. Amer. Bull. 96, 719–730.

Rock, N.M.S., 1988. Numerical geology. Bhattacharji, S., Friedman, G.M., Neugebauer, H.J., Seilacher, A. Lecture notes in the Earth Sciences, vol. 18. Springer-Verlag, Berlin.

Ross, S.M., 1996. Simulation, 2nd edition. Academic Press, New York.

Rowan, J.S., Goodwill, P., 2000. Uncertainty estimation in fingerprinting sediment sources. In: Foster, I.D.L. (Ed.), Tracers in Geomorphology. John Wiley, Chichester, pp. 279–290.

Schlinger, C.M., Veblen, D.R., 1989. Magnetism and transmission electron microscopy of Fe–Ti oxides and pyroxenes in a granulite from Lofoten, Norway. J. Geophys. Res. 94, 14009–14026.

Swiecicki, T., Wilcockson, P., Canham, A., Whelan, G., Homann, H., 1995. Dating correlation and stratigraphy of the Triassic sediments in the West Shetland area. In: Boldy, S.A.R. (Ed.), Permian and Triassic rifting in Northwest Europe, Special Publication-Geological Society, vol. 91, pp. 57–85.

Thompson, R., Oldfield, F., 1986. Environmental Magnetism. Allen and Unwin, London.

Vali, H., von Dobenck, T., Amarantidis, G., Forster, O., Mortenani, G., Bachmann, L., Petersen, N., 1989. Biogeneic and lithogenic magnetic minerals in Atlantic and Pacific deep-sea sediments and their palaeomagnetic significance. Geol. Rundsch. 78, 753–764.

Walden, J., Smith, J.P., Dackombe, R.V., 1996. A comparison of mineral magnetic, geochemical and mineralogical techniques for compositional studies of glacial diamictons. Boreas 25, 115–130.

Walden, J., Oldfield, F., Smith, J.P. (Eds.), Environmental Magnetism: A Practical Guide, Technical Guide, vol. 6. Quaternary Research Association, London.

Walker, T.R., Larson, E.E., Hoblitt, R.P., 1981. Nature and origin of hematite in the Moenkopi Formation (Triassic), Colorado Plateau: a contribution to the origin of magnetism in red beds. J. Geophys. Res. 86, 317–333.

Yu, L., Oldfield, F., 1993. Quantitative sediment source description using magnetic measurements in a reservoir-catchment system near Nijar, S.E. Spain. Earth Surf. Process. Landf. 18, 441–454.